KINEMATIC MODEL OF HIERARCHY STRUCTURE WITH FASCICLES AND LIGAMENT

S. Hirokawa*, T. Hamasaki* and S. Doi*

* Kyushu University/Department of Intelligent Machinery & Systems, Nishi-ku, Motooka 744, Fukuoka, Japan

hirokawa@mech.kyushu-u.ac.jp

Abstract: The stress-strain curve of an industrial composite such as a fiber-reinforced plastic falls between those of fibers and plastic matrix. On the other hand, despite the fact that the biological soft tissue is composed of collagen fascicles in a matrix whose Young's modulus is almost negligible, the Young's modulus of the tissue is higher than the fascicles. To insight into the mechanism of such inverse characteristics, we developed a mathematical model of a ligament, by taking into account a fascicle's kinematic non-uniformity along its longitudinal direction and mechanical interaction between fascicles or a fascicle and matrix. Simulations results demonstrated the inverse characteristics and also helped to understand the mechanism of ligament's failure.

Introduction

The biological soft tissues such as ligaments and tendons have a hierarchial structure composed of collagen fibrils, fibers, fascicles and fascicle bundles. To gain insight into the mechanical properties of the tissues, it may be helpful to elucidate the basic relationships between the microstructures and their mechanical properties in the tissues. In this study, tensile tests were performed on Bone-Ligament-Bone (BLB) units and individual collagen fascicles all from swine Anterior Cruciate Ligaments (ACL) [1]. The relationships between the structures and the mechanical properties for the two kinds of test subject were investigated. The results showed that the BLB's stiffness was higher than the fascicles; Hereafter we will use the word 'stiffness' as the same meaning as a tangent in the stress-strain curve. The same results were reported for a rabitt patellar tendon [2]. However, these results are contrary to the popular notion that because the tissue is composed of collagen fascicles in a matrix whose stiffness is almost negligible, the tissue should not be stiffer than the fascicles that compose it. In fact, the stiffness of an industrial composite such as a fiber-reinforced plastic falls between those of fibers and plastic matrix [3].

So far, the mechanical properties of both the upper- and lower-most levels of the tissue's higharchy such as the colective tissue and the pure fibrils have been fully investigated respectively through the measurement experiments [4], [5] and the model analyses [6], [7]. Yet the mechanical interrelationship between the above two levels is still unclear and the mechanical properties of the submicro-level structure such as the fascicles have not been fully investigated.

To insight into the mechanism of the above-mentioned inverse characteristic in the biological soft tissues, it is crucial not only to measure the mechanical properties in each individual level/element but also to investigate the mechanical interactions among the levels/elements. This approach may also be helpful to undesrstand the mechanism of the tissue's failure. Thus, we performed a mathematical model analysis in which we took into account the affects of interactions between the fascicle-fascicle and fascicle-matrix on the mechanical response of the collective tissue.

Protocol

Figure 1 (a) and (b) show the stress-strain curves of fiber reinforced matrces in the case of respectively the industrial and the biological materials. In Fig.1 (a), a tangent modulus of the stress-strain curve of complex falls between those of fiber and matrix. On the other hand in Fig.1 (b), a tangent modulus of the stress-strain curve of a Bone-ACL-Bone complex exceeds that of fibers, despite the fact that the ACL is composed of collagen fascicles in a matrix whose stiffness is almost negligible. Possible reasons to explain this are reported to be as mechano-chemical interactions between fascicles and/or between fascicles and matrix [2], or contributions from the membranous septa that combines fascicles [1]. However a direct evidence is lacking.

Elements in biological materials are not uniform in size/shape as well as in mechanical properties as compared to those in industorial materials. During the tensile tests on the fascicles, we found that the specimen did not elongate uniformly along its longitudinal direction [1]. Figure 2 and Table 1 show a typical example of the results obtained from our experiments subject to the fascicles of the swine ACL. According to Table 1, the strain value of the total length of the specimen is pretty close to that of segment ③ whose strain value is much larger than those of any other segments. If such is a case, then the stiffness, i.e. stress par unit strain of that specimen would be determined mainly by the

ISSN: 1727-1983

stiffness on the weakest segment no matter how stiff the rest segments are.

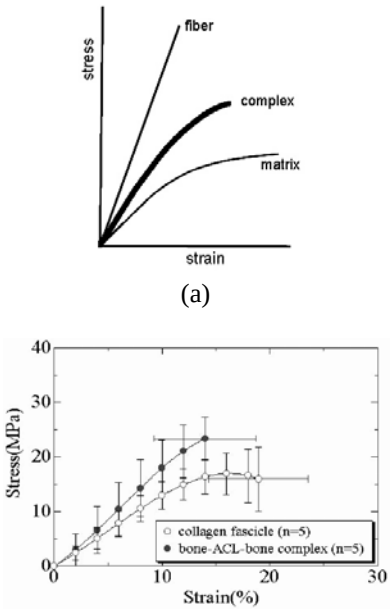

Fig.1 Stress-strain curves of fiber reinforced matrices.
(a) fiber reinforced plastic for the inductorial material,
(b) Anterior Cruciate Ligament from a swine hinder knee joint.

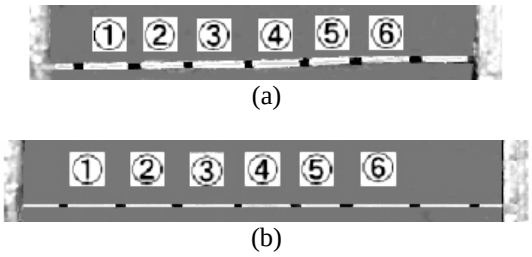

Fig.2 Photographs of a fascicle specimen before and after tensioned indicating non-uniform elongations.
(a) untensioned state, (b) tensioned state

Table 1 Strains along the longitudinal direction of a fascicle specimen.

segment	①	②	③	④	⑤	⑥	total
strain (%)	10.1	7.3	14.6	9.1	4.3	4.3	13.2

It has been thought that the contributions of the matrix or the fascicle-fascicle and fascicle-matrix interactions to the mechanical properties of the tissue are small. But these interactions could play a significant role in surpressing an excessive strain on the weakest segment, thereby resulting in an increase in stiffness of the tissue. As we thought this colud explaine the mechanism of the above-mentioned inverse characteristics in the biological soft tissues, we developed two kinds of mathematical models of ligament; one was a model of ligament as a linear springs' aggregation and the other was a model of ligament as a hyper-elastic continuum. In both the models, we took into account a fascicle's kinematic non-uniformity along its longitudinal direction and we fabricated a virtual spring which represented the effects of fascicle-fascicle and fascicle-matrix interactions on the ligament's stiffness. Then simulations were performed to check if the inverse characteristics were reproduced.

Mathematical Models of Ligament

A model of ligament as a linear springs' aggregation

Figure 3 shows a simple model of the ligament in which two strings represent fascicles and are arranged in parallel, each string is composed of three springs in a row. In each string, one of the three springs is set with a lower spring coefficient than the other two springs to represent a fascicle's kinematic non-uniformity. The mechanical interactions between fascicles or a fascicle and matrix is assumed to be reproduced by a force of a virtual spring, designated as *a cross-link spring* and whose spring constant, c is set further lower than that of the above-mentioned weak spring. It is assumed that the cross-link spring generates a force only in the string's longitudinal direction in proportion to the difference between the longitudinal displacements of two nodes on two strings respectively.

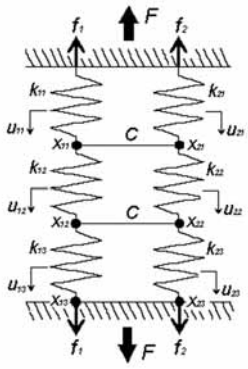

Fig.3 A linear springs' aggregation model of the ligament.

Now, we will extend the simple model shown in Fig.3 to a more general one by increasing the numbers of strings and springs, then we will introduce its kinematic equation. Symbols in Fig.3 indicate as,

suffces i and j: the string's and the spring's numbers respectively,
k_{ij}: a spring constant of the j-th spring on the i-th string,
x_{ij}: a longitudinal coordinate of the j-th node on the i-th string,
u_{ij}: a longitudinal displacement of the j-th node on the i-th string,
c: a spring constant of the cross-link spring,
f_i: a tensile force acting on the i-th string,

ISSN: 1727-1983

F: summation of tensile forces acting on all the strings.

A force equilibrium condition at each node is expressed by the following equation,

$$Au = f \qquad (1)$$

where,

$$\boldsymbol{A} = \begin{bmatrix} a_1 & C_{12} & \cdots & C_{1n} \\ C_{21} & a_2 & \cdots & C_{2n} \\ \vdots & \vdots & \ddots & \vdots \\ C_{n1} & C_{n2} & \cdots & a_n \end{bmatrix}, \quad \boldsymbol{u} = \begin{bmatrix} u_1 \\ u_2 \\ \vdots \\ u_n \end{bmatrix}, \quad \boldsymbol{f} = \begin{bmatrix} f_1 \\ f_2 \\ \vdots \\ f_n \end{bmatrix}$$

$$a_i = \begin{bmatrix} k_{i1}+k_{i2}+c & -k_{i2} & 0 & \cdots & 0 & 0 \\ -k_{i2} & k_{i2}+k_{i3}+c & -k_{i3} & \cdots & 0 & 0 \\ 0 & -k_{i3} & k_{i3}+k_{i4}+c & \cdots & 0 & 0 \\ \vdots & \vdots & \vdots & \ddots & \vdots & \vdots \\ 0 & 0 & 0 & \cdots & k_{in-1}+c & -1 \\ 0 & 0 & 0 & \cdots & k_{in} & 1 \end{bmatrix}$$

$$\boldsymbol{C} = [C_{ij}] = \begin{bmatrix} c & 0 & \cdots & 0 & 0 \\ 0 & c & \cdots & 0 & 0 \\ \vdots & \vdots & \ddots & \vdots & \vdots \\ 0 & 0 & \cdots & c & 0 \\ 0 & 0 & \cdots & 0 & 0 \end{bmatrix}, \quad u_i = \begin{bmatrix} u_1 \\ u_2 \\ \vdots \\ u_{N-1} \\ f_1 \end{bmatrix}, \quad f_i = \begin{bmatrix} (k_{11}-k_{12})l_0 \\ (k_{12}-k_{13})l_0 \\ \vdots \\ k_{1N-1}l_0 \\ k_{1N}(u_{1N}-l_0) \end{bmatrix}$$

Also, the following relation hlds,

$$\sum_{i=1}^{n} f_i = F \qquad (2)$$

For the sake of simplicity, we will assume that along each string, the spring constant of only one spring is set lower than those of the rest springs. We will also assume that the weak spring is allocated at random respectively along each string. Then, we will replace the above-mentioned strings with cylinders of section area A [mm^2] and also we aill assume the cylinders are densely arranged so as to minimize clearance area among them. Figure 4 illustrates the arrangement of the fascicle cylinders and the distribution of weak portions (springs).

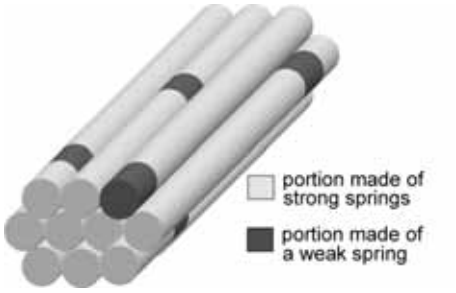

Fig.4 Arrangement of the fascicle cylinders and the distribution of weak portions.

Next, for both the weak and strong springs, we will change their spring constants according to their stretch so as to represent the toe, linear and failure phases seen in a stress-strain curve of the natural ligament. Figure 5 represents a stress-strain curve of the ligament in a linearized form. In the figure, ε_{cs} and ε_{cw} correspond to the strains at which crimps of the fascicles unfold and ε_s and ε_w the strains at failure for the strong and the weak portions respectively. The spring constant of the toe region is set lower than that of the linear region. The spring constant of the failure region is set zero.

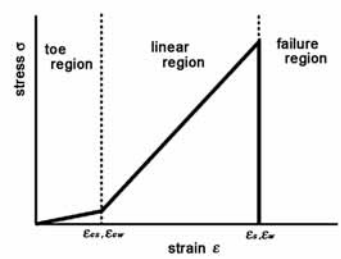

Fig.5 Linearized representation of a stress-strain curve for the natural ligament.

From Fig.5, the relationship between stress σ and strain ε is expressed by the following equation.

$$\sigma = \begin{cases} E_c\varepsilon & \varepsilon < \varepsilon_c \\ E_s - a,\ E_w - b & \varepsilon_c \le \varepsilon \le \varepsilon_s, \varepsilon_w \\ 0 & \varepsilon \ge \varepsilon_s,\ \varepsilon_w \end{cases} \qquad (3)$$

where suffices *s* and *w* show the values for the strong and the weak portions respectively.

Since a weak spring elongates more easily than a strong spring, we will set the strain at which crims unfold and the strain at failue for the weak portion larger than those for the strong portion as,

$$\varepsilon_{cs} < \varepsilon_{cw},\ \varepsilon_s < \varepsilon_w \qquad (4)$$

When the ligament is untensioned, most of the fascicles are straight and arranged in parallel while some are not. Figure 6 (a) shows a microscopic photograph of a longitudinal section of the swine ACL and (b) shows its schematic representation. To incoorporate this cahracteristic into the model, we will assign the different initial lengthes to the different fascicle cylinders.

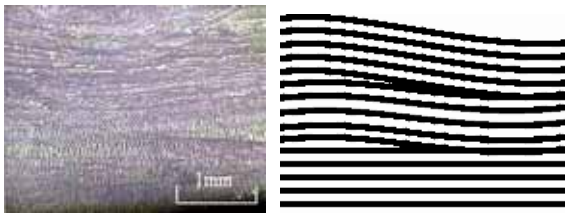

(a) (b)

Fig.6 Fascicle arrangements on the longitudinal section of the swine ACL.
(a) microscopic photograph (b) shematic representation

A model of ligament as a hyprer-elastic continuum

We create a 2D continuous model of the ligament under the conditions that the fascicle is made of non-isotropic hyper-elastic material and the matrix is fabricated to be assumed Mooney-Rivlin material

ISSN: 1727-1983

whose stiffness is much lower than that of the fascicle material. Figure **7** shows a simple model of ligament in which two strips corresponding to fascicles are arranged in parallel, each strip is composed of three segments. The matrix is also represented a narrow strip of three segments and it is sandwitched with the fascicle strips.

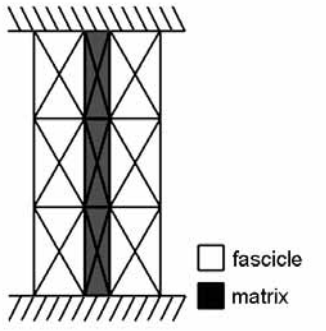

Fig.7 A hyprer-elastic continuum model of ligament.

First, a 2D constitutive equation for the fascicle is introduced as,

$$\dot{\sigma} = \boldsymbol{C}_e \boldsymbol{D}$$

$$\begin{bmatrix} \dot{\sigma}_x \\ \dot{\sigma}_y \\ \dot{\sigma}_{xy} \end{bmatrix} = \begin{bmatrix} C_{xx} & C_{xy} & 0 \\ C_{yx} & C_{yy} & 0 \\ 0 & 0 & \Gamma \end{bmatrix} \begin{bmatrix} D_x \\ D_y \\ 2D_{xy} \end{bmatrix} = \frac{1}{(1-\nu_x\nu_y)} \begin{bmatrix} E_x & E_x\nu_y & 0 \\ E_y\nu_x & E_y & 0 \\ 0 & 0 & \Gamma \end{bmatrix} \begin{bmatrix} D_x \\ D_y \\ 2D_{xy} \end{bmatrix} \quad (5)$$

where, $\dot{\sigma}$ is the velocity of Cauchy stress, $\boldsymbol{C}_e$ is the elasticity coefficient tensor and $\boldsymbol{D}$ is the deformation velocity tensor. E_x, E_y, ν_x, and ν_y are the Young's modulus and the Poisson ratio for respectively x and y diretions. Γ is a mudulus of transverse elasticity.

Next, we will introduce a constitutive equation for the matrix. A strain energy function for the Mooney-Rivlin material is given by,

$$W = \alpha(I_1 - 3) + \beta(I_2 - 3) + h(I_3 - 1) \quad (6)$$

where, α, β are the Mooney-Rivlin constants, h is hydrostatic pressure and I_1, I_2 and I_3 are the invariants of right Cauchy-Green deformation tensor.

The Kirchhoff stress tensor $\boldsymbol{S}$ is expressed with the strain energy function $\boldsymbol{W}$ and the Green strain tensor $\boldsymbol{G}$ as,

$$\boldsymbol{S} = \frac{\partial \boldsymbol{W}}{\partial \boldsymbol{G}} = \alpha \frac{\partial \boldsymbol{I}_1}{\partial \boldsymbol{G}} + \beta \frac{\partial \boldsymbol{I}_2}{\partial \boldsymbol{G}} + h \frac{\partial \boldsymbol{I}_3}{\partial \boldsymbol{G}} \quad (7)$$

Then, the constitutive equation of matrix is simply given as,

$$\boldsymbol{S} = \boldsymbol{C}^m \boldsymbol{G} \quad (8)$$

As a plane stress is considered here, the following relations hold,

$$S_{13} = S_{31} = S_{23} = S_{32} = S_{33} = 0 \quad (9)$$

Next, we will express the constitutive equations by incremental forms. Then for the fascicle, Eq.(5) is rerwitten as,

$$\Delta \dot{\sigma} = C^e \Delta D \quad (10)$$

and for the matrix, Eq.(8) is rewritten as,

$$\Delta S = C^m \Delta G \quad (11)$$

Finally, we will derive the stiffness equation for the collective ligament including the fascicles and the matrix by using the principal of virtual work, whose incremental form is given by,

$$\int_{V_0} \left(\sigma_{ji} + \Delta \Pi_{ji}\right) \frac{\partial \delta u_i}{\partial X_j} dV_0 = \int_{S_{0t}} (\bar{t}_0 + \Delta \bar{t}_0) \cdot \delta u dS_0 \quad (12)$$

where, $\Delta \Pi_{ji}$ is an increment of the nominal stress, $\bar{t}_0$ and $\Delta \bar{t}_0$ are the surface force and its increment respectively, σ_{ji} is Cauchy stress.

By representing the ligament's shape by flat triangular elements and substitutig Eqs (10) and (11) into Eq.(12), we obtain the following stiffness equation,

$$\boldsymbol{K} \Delta \boldsymbol{u} = \boldsymbol{f} \quad (13)$$

This completes the formulation of the problem.

Simulations and Results

The linear springs' aggregation model

In the simulation for the linear springs' aggregation model, we set the number of strings (cylinders) as 50 and each strings was made of 10 springs. The parameter values used in the simulation are shown in Table 2.

Table 2 Parameter values used for the linear springs' aggregation model.

parameter	symbol	value
Fascicle		
Young's modulus	E_s, E_w	260, 40 [Mpa]
section area	A	0.07 [mm^2]
initial length	ℓ_0	5.2 [mm]
strain of crimp	ε_{cs}, ε_{cw}	3, 4 [%]
ratio of the Young's modulus in the toe region relative to that in the linear region	q	10 [%]
failure strain	ε_s, ε_w	15, 30 [%]
Matrix		
spring constant	c	5000 [N/m]

We set the ratio between the Young's moduli in the toe and linear regions as q. Thus the Young's moduli in the toe region for respectively strong and weak segments E_{cs}, E_{cw} were introduced as,

$$\begin{cases} E_{cs} = \frac{q}{100} \times E_s \\ E_{cw} = \frac{q}{100} \times E_w \end{cases} \quad (14)$$

Simulations were performed under such conditions as our linear springs' aggregation model was made of,

(a) the springs of the same initial length, without the cross-link springs

ISSN: 1727-1983

(b) the springs of the same initial length, with the cross-link springs,
(c) the springs of the various initial lengthes, with the cross-link springs.

Condition (a) is vertually same as the case of a single spring. Conditions (b) and (c) correspond to a collective ligament composed of fascicles' bundles. Still (c) was employed from the fact that for the natural ligament all the fascicles do not stretch nor shear the tensile force equally when the ligament is pulled.

The simulation results are shown in Fig.8. In the figure, the tangents of stress-strain curves for conditions (b) and (c) with the cross-link springs are almost same with each other, and are steeper than that of condition (a) without the cross-link springs. We found that the stress-strain curve of condition (a) was identical to that of a single string. It should be noted that a phase of microstructure failure is clearly drawn for condition (c) in which the springs have various initial lengthes.

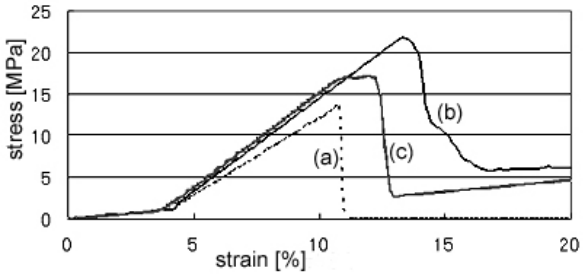

Fig.8 Stress-strain courves for the various types of linear springs' aggregation models (Legends (a), (b) and (c) are explained in the text).

The hyper-elastic continuum model

In the simulation for the hyper-elastic continuum model, ten strips representing fascicles were arranged in parallel, and nine narrow strips representing the matrix were sandwiched between them so as to represent a belt-shape ligament. Each of the fascicle and matrix strips was divided by 10 segments along its longitudinal direction; each segment was further devided into 4 triangular meshes for the FEM analysis. Alon each fascicle strip, one segment was set lower with its Young's modulus than the rest nine segments. The parameter values used in the simulation are shown in Table 3.

Table 3 Parameter values used for the hyper-elastic continuum model.

parameter	symbol	value
Fascicle		
Young's modulus	E_{ys}, E_{yw}	260, 40 [Mpa]
Poisson's ratio (x)	μ_{xs}, μ_{xw}	0.3
Poisson's ratio (y)	μ_{ys}, μ_{yw}	0.5
shear modulus	G_s, G_w	1, 0.3 [Gpa]
Matrix		
constants of Mooney-Rivlin material	α, β	1, 0.1 [Mpa]
Fascicle and Matrix Composite		
thickness	t	0.1 [mm]

Simulations were performed under such conditions as the model was made of,

(a) weak segments were randomly arranged, without matrix,
(b) weak segments were aligned side by side, with matrix,
(c) weak segments were randomly arranged, with matrix.

Condition (c) represented most likely the natural ligament, and conditions (a) and (b) were employed for comparison.

The simulation results are shown in Fig.9 through 11. Figure 9 shows the stress-strain curves for the above-mentioned three conditions (a) through (c). We found that when the weak segments were aligned side by side (condition (b)), the tangent of stress-strain curve became equivalent to those without matrix (condition (a)). In the case when the weak segments were randomly arranged and the matrix was incooprated (condition (c)), the tangent of stress-strain curve became higher than the other two conditions.

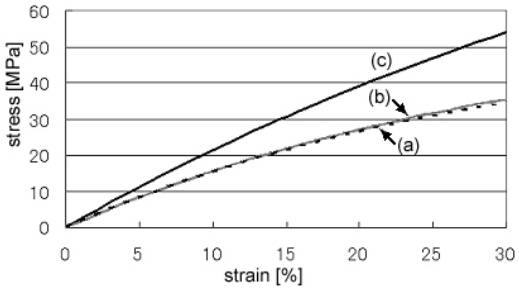

Fig.9 Stress-strain courves for the various types of hyper-elastic continuum models (Legends (a), (b) and (c) are explained in the text. Same as Figs.10 and 11).

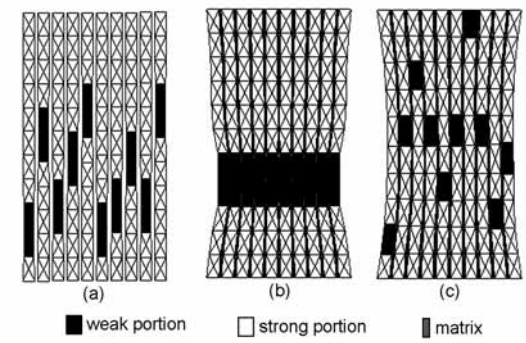

Fig.10 Deformed shapes under 30% stretch.

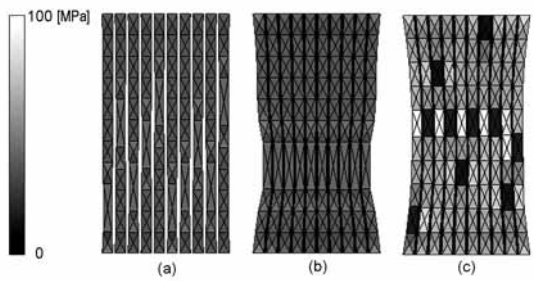

Fig.11 Principal stress distribution maps under 30% stretch.

ISSN: 1727-1983

Figure 10 and 11 show the deformed shapes and the principal stress distribution maps respectively when the model was stretched by 30%. Contribution of the matrix is seen in the deformed shapes of Fig.11 (b) and (c). It should be noted that the strong segment next to the weak segment exhibits high stress so that the weak segment is not excessively stretched as shown in Fig.11 (c).

Discussion

The linear springs' aggregation model

The simulation results of our linear springs' aggregation model clearly demonstrated that the tangnt modulus of the stress-strain curve for the collective ligament became higher than that of the fascicles. It should be noted that during tensile test of a single fascicle, excessive elongation would be exerted at the weakest portion along the fascicle. Then we may mislead that the elongation is exerted along the total length of the fascicle, and may underestimate the stiffness of the fascicle, even though the stiffness of the most part of the fascicle is much higher. We believe the matrix or the fascicle-fascicle and fascicle-matrix interactions contribute to surpress excessive strain on the weak portion, resulting in increase in stiffness of the ligament. Our cross-link spring demonstrated the role of the above-mentioned interactions.

For the sake of simplicity we employed only two kinds of spring constants. Springs with various spring constants should be employed and allocated basing upon the statistics from the experimental data in oder to make the model more realistic.

As shown in Fig.8, our simulation results clearly represented the three phases seen in a stress-strain curve of the natural ligament. In the case of (c) i.e. a model with the springs of the various initial lengthes and with the cross-link springs, the shape of the stress-strain curve around the failure phase duplicated that of the natural ligament; indicating a successive rupture of fascicles, and a laxity state of the ligament.

The hyper-elastic continuum model

The inverse characteristic between the fascicle and the collective ligament was reproduced in the simulation for the hyper-elastic continuum model as well. We set the stiffness of the matrix much lower than that of the fascicle. Neverthless the matrix contributes to surpress excessive strain on the weak segment as the cross-link springs do in the linear springs' aggregation model. From Fig.9, we found that high stresses were exerted on the strong segments which adjoin the weak segments. Thus we may introduce such an important conclusion that a ligament's failure could initiate on those *strong* segments.

In our hyper-elastic continuum model, yet three phases in the stress-strain characteristic have not been reproduced, the validity for the parameter values used in the simulation have not been verified either. These are the problems to be solved in our future study.

Conclusion

We have developed two mathematical models of the ligament to explain how the ligament can be stiffer than the fascicles which must be stiffest in the ligament. In both the models, we took into account the mechanical non-uniformity of the fascicle along its longitudinal direction and the contribution of interactions between the fascicle-fascicle and the fascicle-matrix against the elongation of the fascicle. Simulation results from both the models demonstrated that the tangnt modulus of the stress-strain curve for the collective ligament became higher than that of the fascicles. The results may help to understand the mechanism of ligament's failure.

References

[1] Hirokawa, S., and Sakoshita, S.: 'An Experimental Study of the Microstructures and Mechanical Properties of Swine Cruciate Ligaments', *Japanese Socity of Mechanical Engineers, International Journal of Bioengineering*, Series C, 45, 2003, p.1417-1425.

[2] MIYAZAKI, H., and HAYASHI, K.: 'Tensile Tests of Collagen Fibers Obtained from the Rabbit Patellar Tendon', *Biomedical Microdevices*, **2**, 1999, p.151-157.

[3] NIKI, E., and TAJIRI, M.: 'Reinforcement Mechanism of Fiber Composite Materials, *Ceramics* (in Japanese), **4**, 1969, p.490-495.

[4] BUTLER, D.L., GUAN, Y., CUMMINGS, J. F., FEDER, S. M., and LEVY, M. S.: 'Location-dependent variations in the material properties of the anterior cruciate ligament', *J. Biomechanics*, **25**, 1992, p.511-518.

[5] SILVER, F.H., JOSEPH, W.F. and GURINDER, P.S.: 'Collagen self-assembly and the development of tendon mechanical properties', *J. Biomechanics*, **36**, 2003, p.1529-1553.

[6] WOO, S.L-Y., JOHNSON, G.A. and SMITH, B.A.: 'Mathematical Modeling of Ligaments and Tendons', *J. Biomechanical Engineering*, **115**, 1993, p.468-473.

[7] LANIR, Y.: 'A Microstructure Model for the Rheology of Mammmalian Tendon', *J. Biomechanical Engineering*, **102**, 1980, p.332-339.

ISSN: 1727-1983